

# Magnetism of the antiferromagnetic spin- $\frac{1}{2}$ tetramer compound CuInVO<sub>5</sub>

Masashi Hase<sup>1</sup> \* Masahige Matsumoto<sup>2</sup>, Akira Matsuo<sup>3</sup>, and Koichi Kindo<sup>3</sup>

<sup>1</sup>*National Institute for Materials Science (NIMS), Tsukuba, Ibaraki 305-0047, Japan*

<sup>2</sup>*Department of Physics, Shizuoka University, Shizuoka 422-8529, Japan*

<sup>3</sup>*The Institute for Solid State Physics (ISSP), the University of Tokyo, Kashiwa, Chiba 277-8581, Japan*

(Dated: September 4, 2018)

We measured the temperature dependence of the magnetic susceptibility and specific heat and the magnetic-field dependence of the magnetization of CuInVO<sub>5</sub>. An antiferromagnetically ordered state appears below  $T_N = 2.7$  K. We observed a  $\frac{1}{2}$  quantum magnetization plateau above 30 T at 1.3 K. We show that the spin system consists of antiferromagnetic spin- $\frac{1}{2}$  tetramers with  $J_1 = 240 \pm 20$  and  $J_2 = -142 \pm 10$  K for the intratetramer interactions.

PACS numbers: 75.10.Jm, 75.50.Ee, 75.40.Cx, 75.47.Lx

## I. INTRODUCTION

The interacting antiferromagnetic (AF) spin-dimer compounds TlCuCl<sub>3</sub> [1–5] and KCuCl<sub>3</sub> [6, 7] show a pressure-induced or magnetic-field-induced magnetic quantum phase transition. Experimental observations [8–11] and the theoretical background [12, 13] of massive longitudinal-mode magnetic excitations in the ordered state were reported for these compounds. The longitudinal mode and massless transverse modes (Nambu-Goldstone modes) [14] are related to fluctuations in the amplitude and phase of the order parameter, respectively. The longitudinal mode is the analog of the Higgs particle [15–17].

According to the results of theoretical investigations, the longitudinal mode can exist in interacting AF spin cluster systems that are realized in Cu<sub>2</sub>Fe<sub>2</sub>Ge<sub>4</sub>O<sub>13</sub> and Cu<sub>2</sub>Cd<sub>2</sub>B<sub>6</sub> [18]. The spin systems in Cu<sub>2</sub>Fe<sub>2</sub>Ge<sub>4</sub>O<sub>13</sub> [18] and Cu<sub>2</sub>Cd<sub>2</sub>B<sub>6</sub> [19–21] can be regarded as interacting AF spin tetramers (Fe-Cu-Cu-Fe and Cu-Cu-Cu-Cu tetramers, respectively). The shrinkage of ordered magnetic moments by quantum fluctuation is important for the appearance of the longitudinal mode. The ground state (GS) can be a spin-singlet state in isolated AF spin clusters. Therefore, some interacting spin cluster systems are advantageous for the longitudinal mode. An antiferromagnetically ordered state appears in Cu<sub>2</sub>Fe<sub>2</sub>Ge<sub>4</sub>O<sub>13</sub> [22] and Cu<sub>2</sub>Cd<sub>2</sub>B<sub>6</sub> [19] in zero magnetic field under atmospheric pressure. The magnetic excitations in Cu<sub>2</sub>Fe<sub>2</sub>Ge<sub>4</sub>O<sub>13</sub> have been investigated by inelastic neutron scattering (INS) experiments on single crystals [22–25]. The longitudinal mode was not confirmed because of the small INS intensities due to the large excitation energies (> 15 meV) and because of the overlap of the transverse modes. The magnetic excitations in Cu<sub>2</sub><sup>114</sup>Cd<sup>11</sup>B<sub>2</sub>O<sub>6</sub> were studied by INS experiments on its powder [21]. Although the results suggest the existence of the longitudinal mode, there was no conclusive evidence because powder was used. A single crystal suit-

able for the measurements of physical properties has not been reported.

We require further spin cluster compounds that have an antiferromagnetically ordered state and low-energy longitudinal-mode magnetic excitations. We focus on spin- $\frac{1}{2}$  tetramers because of the following magnetism. The Hamiltonian of a spin tetramer is expressed as

$$\mathcal{H} = J_1 S_2 \cdot S_3 + J_2 (S_1 \cdot S_2 + S_3 \cdot S_4). \quad (1)$$

When  $J_1 > 0$  or  $J_2 > 0$ , the GS is the spin-singlet state. Therefore, the shrinkage of ordered moments can be expected in an ordered state generated by the introduction of intertetramer interactions. The ordered state is possible under the condition that the value of  $\Delta$  is comparable to or less than that of an effective intercluster interaction [18]. Here  $\Delta$  is the energy difference (spin gap) between the singlet GS and first-excited triplet states. The effective intercluster interaction is given by the sum of the products of the absolute value of each intercluster interaction ( $|J_{\text{int},i}|$ ) and the corresponding number of interactions per spin ( $z_i$ ) as  $J_{\text{eff}} = \sum_i z_i |J_{\text{int},i}|$ . The effective intercluster interaction is usually much smaller than the dominant intraclusster interactions. Therefore,  $\Delta$  should be much smaller than the dominant intraclusster interactions for the appearance of the ordered state. Figure 1 shows the eigenenergies of the excited states measured from the GS in an isolated spin- $\frac{1}{2}$  tetramer [26]. As shown in Fig. 1(a) for  $J_1 > 0$ ,  $\Delta/J_1$  can be sufficiently small when  $J_2$  has negative or small positive values. Even under a small  $J_{\text{eff}}$ , an ordered state is expected in a spin-tetramer compound for  $J_1 > 0$  and  $J_2 < 0$ . The small  $\Delta/J_1$  is in contrast to  $\Delta/J = 1$  in the AF spin- $\frac{1}{2}$  dimer given by  $JS_1 \cdot S_2$ . As shown in Fig. 1(a), the GS and first-excited states are well separated from the other excited states (ESs). This means that the low-energy physics can be described by an effective spin-dimer (singlet-triplet) system [18].

We can expect spin- $\frac{1}{2}$  tetramers in CuInVO<sub>5</sub> from its crystal structure [27]. The Cu<sup>2+</sup> ions ( $3d^9$ ) have localized spin- $\frac{1}{2}$ . The positions of the Cu ions and the O ions connected to the Cu ions are shown schematically in Fig. 2(a). Two crystallographic Cu sites (Cu1 and Cu2) exist. Red and blue bars indicate the shortest and

\*Electronic address: HASE.Masashi@nims.go.jp

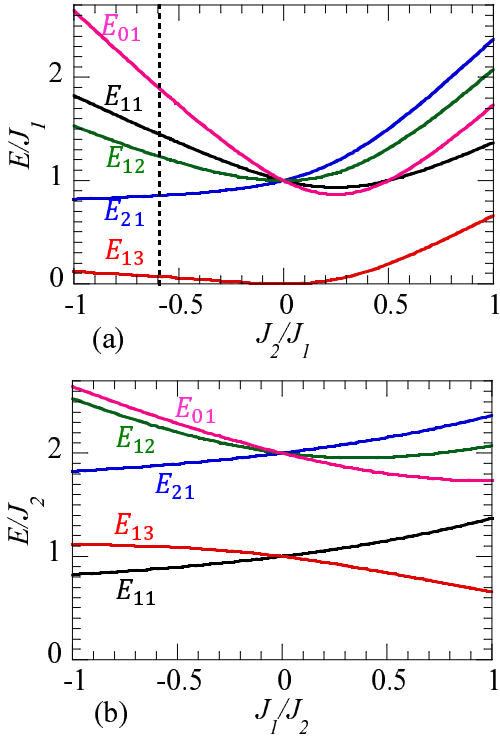


FIG. 1: (Color online) Eigenenergies of excited states measured from the ground state in an isolated spin- $\frac{1}{2}$  tetramer expressed by Eq. (1). There are two  $S^T = 0$  states ( $|01\rangle$  and  $|02\rangle$ ), three  $S^T = 1$  states ( $|11\rangle$ ,  $|12\rangle$ , and  $|13\rangle$ ), and one  $S^T = 2$  state ( $|21\rangle$ ).  $S^T$  is the value of the sum of the spin operators in the tetramer. The eigenstates  $|ij\rangle$  of the isolated tetramer are explicitly given in [26]. In the isolated tetramer, the ground state is the spin-singlet  $|02\rangle$  state. (a)  $J_1 > 0$ . The vertical dashed line indicates the  $J_2/J_1$  value of CuInVO<sub>5</sub> evaluated in the present work. (b)  $J_2 > 0$ .

second-shortest Cu-Cu bonds, respectively. The Cu-Cu distances at room temperature are 3.117 and 3.173 Å, respectively. The shortest bond has two identical Cu1-O-Cu1 paths whose angle is 89.75°. The second-shortest bond has two different Cu1-O-Cu2 paths with angles of 107.61 and 88.19°. The Cu-Cu distances in the other bonds are 4.705 Å or greater. If dominant exchange interactions exist in the shortest and second-shortest Cu-Cu bonds, spin tetramers given by Eq. (1) are formed. Figure 2(b) shows the arrangement of the spin tetramers. Two types of tetramers (I and II) exist, although they are equivalent to each other as a spin system. In this paper, we report the magnetism of CuInVO<sub>5</sub>. An AF long-range order appears below  $T_N = 2.7$  K. We show that the spin system consists of spin tetramers with  $J_1 > 0$  and  $J_2 < 0$ .

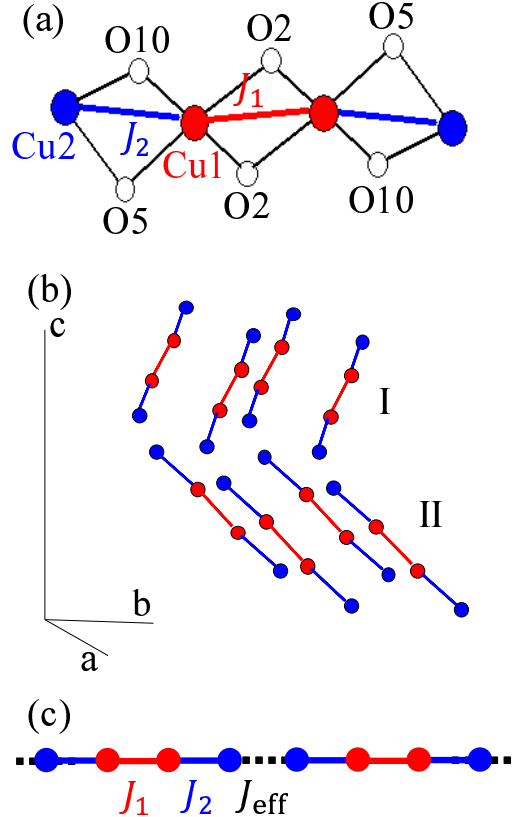


FIG. 2: (Color online) (a) Schematic drawing of positions of Cu<sup>2+</sup> ions having spin- $\frac{1}{2}$  and O<sup>2-</sup> ions connected to Cu<sup>2+</sup> ions in CuInVO<sub>5</sub>. Red, blue, and white circles indicate Cu1, Cu2, and O sites, respectively. Red and blue bars represent the shortest and second-shortest Cu-Cu bonds, respectively. Thin black bars represent Cu-O bonds. We define  $J_1$  and  $J_2$  as the exchange interaction parameters for the shortest and second-shortest Cu-Cu bonds, respectively. The  $J_1$  and  $J_2$  interactions form a spin- $\frac{1}{2}$  tetramer. (b) Schematic drawing of spin tetramers in CuInVO<sub>5</sub>. Two types of tetramers (I and II) exist, although they are equivalent to each other as a spin system. The space group of CuInVO<sub>5</sub> is  $P2_1/c$  (No. 14). The lattice constants at room temperature are  $a = 8.793(2)$ ,  $b = 6.1542(6)$ ,  $c = 15.262(2)$  Å,  $\beta = 106.69(2)$ °, and  $Z = 8$  (8 formulas per unit cell) [27]. (c) Interacting spin tetramer model used to calculate magnetization using a mean-field theory based on the tetramer unit (tetramer mean-field theory).

## II. EXPERIMENTAL AND CALCULATION METHODS

Crystalline CuInVO<sub>5</sub> powder was synthesized by a solid-state reaction at 1,023 K in air for 100 h with intermediate grindings. We confirmed the formation of CuInVO<sub>5</sub> using an x-ray diffractometer (RINT-TTR III; Rigaku). We measured the specific heat using a Physical Property Measurement System (PPMS; Quantum Design). We measured the magnetization in magnetic fields of up to 5 T using a superconducting quantum inter-

ference device (SQUID) magnetometer Magnetic Property Measurement System (MPMS; Quantum Design). High-field magnetization measurements were conducted using an induction method with a multilayer pulsed field magnet installed at the Institute for Solid State Physics (ISSP), the University of Tokyo.

We obtained the eigenenergies and eigenstates of isolated spin- $\frac{1}{2}$  tetramers using an exact diagonalization method [26]. We calculated the temperature  $T$  dependence of the magnetic susceptibility and the magnetic-field  $H$  dependence of the magnetization  $M(H)$  using the eigenenergies and eigenstates. We calculated  $M(H)$  for the model shown in Fig. 2(c) using a mean-field theory based on the tetramer unit (tetramer mean-field theory). Finite magnetic moments were initially assumed on the Cu sites in the tetramer. The mean-field Hamiltonian was then expressed by a  $16 \times 16$  matrix form under consideration of the external magnetic field and the molecular field from the nearest-neighbor sites. The eigenstates of the mean-field Hamiltonian were used to calculate the expectation value of the ordered moments on the Cu sites. We continued this procedure until the values of the magnetic moments converged. We finally obtained a self-consistently determined solution for  $M(H)$ .

### III. RESULTS AND DISCUSSION

The red circles in Figs. 3 and 4 show the  $T$  dependence of the specific heat  $C(T)$  of  $\text{CuInVO}_5$  in zero magnetic field and the magnetic susceptibility  $\chi(T)$  in a magnetic field of  $H = 0.01$  T, respectively. We can observe a peak in  $C(T)$  at 2.7 K and a clear decrease in  $\chi(T)$  below this temperature, indicating the occurrence of an AF long-range order. A broad maximum can be seen around 8 K in  $C(T)$  and around 11 K in  $\chi(T)$ , indicating that the origin of the broad maximum in  $C(T)$  is magnetic [28]. As  $T$  is increased,  $\chi(T)$  decreases rapidly up to  $T = 40$  K then decreases slowly at higher temperatures. Other phase transitions were not observed in  $C(T)$  and  $\chi(T)$  below 300 K.

The thick red lines in Figs. 5(a) and (b) show the  $H$  dependence of the magnetization  $M(H)$  of  $\text{CuInVO}_5$  measured at 1.3 and 30 K, respectively. We can observe a  $\frac{1}{2}$  quantum magnetization plateau above 30 T at 1.3 K. The  $g$  value was evaluated to be  $2.09 \pm 0.02$  from the magnetization of the plateau. The magnetization plateau is smeared at 30 K.

We compare  $\chi(T)$  and  $M(H)$  for  $\text{CuInVO}_5$  with those calculated for isolated spin tetramers. The green line in Fig. 4(b) indicates  $\chi(T)$  calculated for an isolated spin tetramer with  $J_1 = 240$  and  $J_2 = -142$  K. The  $J_1$  and  $J_2$  values are listed in Table I. The agreement between the experimental and calculated  $\chi(T)$  is nearly perfect above 30 K, whereas a discrepancy is seen below 30 K. The black lines in Fig. 5 indicate  $M(H)$  calculated for an isolated spin tetramer with the same  $J_1$  and  $J_2$  values. The calculated  $M(H)$  is similar to the experimental

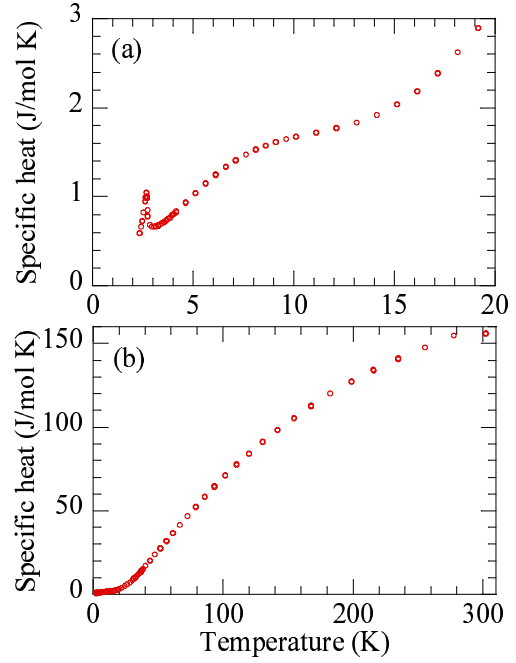


FIG. 3: (Color online) Temperature  $T$  dependence of the specific heat  $C(T)$  of  $\text{CuInVO}_5$  in zero magnetic field.

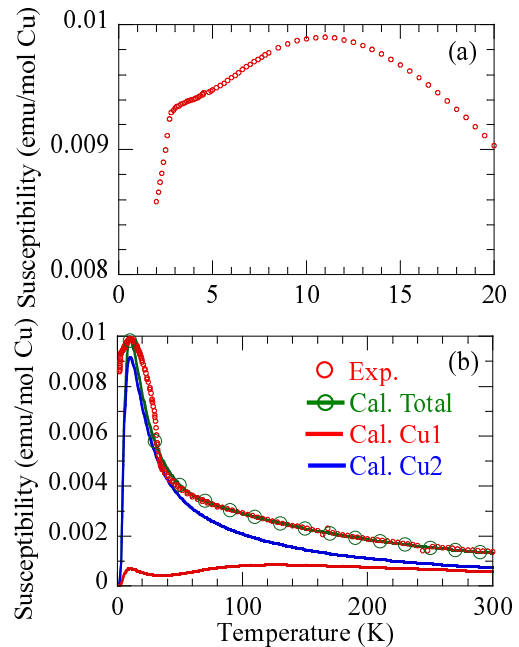


FIG. 4: (Color online) Temperature  $T$  dependence of the magnetic susceptibility  $\chi(T)$  of  $\text{CuInVO}_5$  (circles) in a magnetic field of  $H = 0.01$  T. Green, red, and blue lines indicate  $\chi(T)$  calculated for the total, Cu1, and Cu2 spins, respectively, in an isolated spin- $\frac{1}{2}$  tetramer. The  $J_1$  and  $J_2$  values are listed in Table I.

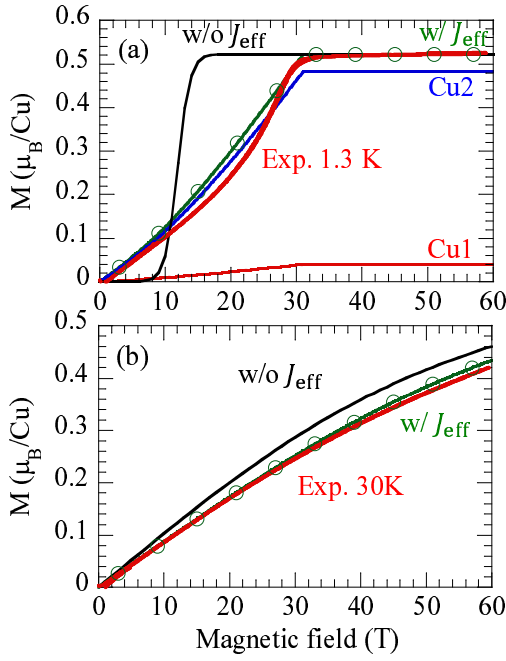


FIG. 5: (Color online) Magnetic-field dependence of the magnetization of  $\text{CuInVO}_5$  (thick red lines). Green, red, and blue lines indicate the magnetization calculated for the total, Cu1, and Cu2 spins, respectively, in the interacting spin- $\frac{1}{2}$  tetramer model in Fig. 2(c). Black lines indicate the magnetization calculated for an isolated spin- $\frac{1}{2}$  tetramer. The values of the exchange interactions are listed in Table I. (a) Magnetization at 1.3 K. (b) Magnetization at 30 K.

$M(H)$  at 30 K, whereas the isolated spin tetramer model fails to reproduce the experimental  $M(H)$  at 1.3 K.

The agreement between the experimental and calculated results above 30 K indicates that the spin system in  $\text{CuInVO}_5$  consists of spin tetramers with  $J_1 = 240$  and  $J_2 = -142$  K. To stabilize the ordered state, intertetramer interactions must exist in  $\text{CuInVO}_5$ . Intertetramer interactions have a greater effect on the magnetization at lower  $T$ . Therefore, the discrepancy between the experimental results and those calculated for the isolated spin tetramer appears at low  $T$ . The magnetic structure of  $\text{CuInVO}_5$  has not yet been reported. It is difficult to determine which intertetramer interactions are effective. Therefore, we assumed the simple model shown in Fig. 2(c) and calculated  $M(H)$  using the tetramer mean-field theory. Since multiple intertetramer interactions are expected in  $\text{CuInVO}_5$ ,  $J_{\text{eff}}$  is the effective interaction between tetramers. As described below, the magnetic moment on Cu1 sites is small in the spin tetramer with  $J_1 = 240$  and  $J_2 = -142$  K. Therefore, we assumed intertetramer interactions between Cu2 spins. The green lines in Fig. 5 indicate  $M(H)$  calculated for the interacting spin tetramer with  $J_1 = 240$ ,  $J_2 = -142$ , and  $J_{\text{eff}} = 30$  K. The experimental and calculated magnetizations are in agreement with each other at both 1.3

TABLE I: Values of exchange interaction parameters and  $g$  value. We used the central values for the calculations of the magnetic susceptibility in Fig. 4, the magnetization in Fig. 5, and the eigenenergies in Fig. 6.

$J_1$ (K)	$J_2$ (K)	$J_{\text{eff}}$ (K)	$g$
$240 \pm 20$	$-142 \pm 10$	$30 \pm 4$	$2.09 \pm 0.02$

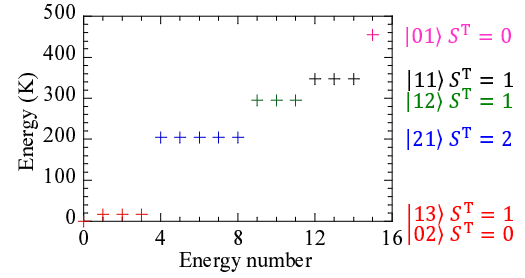


FIG. 6: (Color online) Eigenenergies of the excited states measured from the ground state ( $|02\rangle$  state) in the isolated spin- $\frac{1}{2}$  tetramer expressed by Eq. (1). The  $J_1$  and  $J_2$  values are listed in Table I.

and 30 K.

Figure 6 shows the eigenenergies of the excited states measured from the GS ( $|02\rangle$  state) in the isolated spin tetramer with  $J_1 = 240$  and  $J_2 = -142$  K. The first excited states are the spin-triplet  $|13\rangle$  states located at  $\Delta = 17$  K. The condition for the appearance of the ordered state ( $\Delta \leq J_{\text{eff}}$ ) is satisfied. The second excited states are the spin-quintet  $|21\rangle$  states located at 205 K. The large energy difference between the first and second ESSs generates the  $\frac{1}{2}$  quantum magnetization plateau in Fig. 5(a).

We roughly estimated the errors of the  $J_1$ ,  $J_2$ , and  $J_{\text{eff}}$  values and listed them in Table I. A discrepancy between the experimental and calculated  $\chi(T)$  appears around 80 K when  $J_1$  deviates from 240 K. The experimental and calculated  $\chi(T)$  are not in agreement with each other when  $J_1 = 220$  or 260 K. A discrepancy between the experimental and calculated  $\chi(T)$  appears around 11 K when  $J_2$  deviates from -142 K. The peak heights of the experimental and calculated  $\chi(T)$  are not in agreement with each other when  $J_2 = -132$  or -152 K. The magnetic field at which the  $1/3$  magnetization plateau appears increases with increasing  $J_{\text{eff}}$ . We roughly estimated the error of  $J_{\text{eff}}$  to be  $\pm 4$  K.

The results calculated for spins on the Cu1 and Cu2 sites are shown in Figs. 4(b) and 5(a). We used the isolated and interacting spin tetramers in the calculations of  $\chi(T)$  and  $M(H)$ , respectively. Cu2 spins show much larger magnetization than Cu1 spins at low  $T$ . The maximum  $\chi(T)$  around 11 K and the rapid decrease up to  $T = 40$  K mainly originate from the Cu2 spins. As  $T$  is increased further, the susceptibility of Cu1 spins in-

creases up to  $T = 130$  K, whereas that of Cu2 spins decreases. Therefore, the total susceptibility shows weak  $T$  dependence between 50 and 100 K. The most dominant interaction is the  $J_1$  interaction. The spin state of Cu1 spins is similar to the singlet state in AF dimers [29–31]. Therefore, the magnetization of Cu1 spins is small at low  $T$ . The two Cu2 spins in a tetramer are weakly and antiferromagnetically coupled to each other through a Cu1-Cu1 dimer in the same tetramer. Thus, the magnetization of Cu2 spins is large. The susceptibility and magnetization of CuInVO<sub>5</sub> resemble those of Cu<sub>3</sub>(P<sub>2</sub>O<sub>6</sub>OH)<sub>2</sub>, which has spin- $\frac{1}{2}$  trimerized chains expressed as the sequence -Cu(1)-Cu(2)-Cu(2)- [32, 33]. The AF exchange interaction is largest between two neighboring Cu(2) spins (111 K). The magnetization of Cu(2) spins is small at low  $T$ . In each chain, two Cu(1) spins are weakly coupled to each other through an intermediate Cu(2)-Cu(2) AF dimer. The magnetization of Cu(1) spins is large.

In CuInVO<sub>5</sub>, the low-energy triplet excitation is expected to have a finite gap above  $T_N$  as in Cu<sub>2</sub>CdB<sub>2</sub>O<sub>6</sub> [21]. When the temperature is decreased, the gap closes at  $T_N$  and the triplet excitation splits into a longitudinal mode and twofold degenerate transverse modes at  $T < T_N$ . Slightly below  $T_N$ , the ordered moment is small and the longitudinal mode is expected to be in the low-energy region (on the order of 1 meV). Thus, the ordered phase in CuInVO<sub>5</sub> corresponds to the pressure-induced ordered phase in TlCuCl<sub>3</sub> [1, 2, 9, 10, 12] and KCuCl<sub>3</sub> [6, 11]. CuInVO<sub>5</sub> may be useful for studying the longitudinal mode under the atmospheric pressure.

The magnetic structure is necessary to calculate magnetic excitations. In future, we will determine the magnetic structure of CuInVO<sub>5</sub> by neutron powder diffraction experiments. Although <sup>115</sup>In atoms (natural abundance 95.7 %) strongly absorb neutrons [the thermal absorption cross section is 202(2) barn for 0.0253 eV], it is expected to be possible to obtain diffraction patterns to determine the magnetic structure using a double-wall container. It is difficult to observe magnetic excitations by INS experiments because of the strong neutron absorption by <sup>115</sup>In atoms. We intend to form single crystals of CuInVO<sub>5</sub> and perform Raman scattering experiments on them. We expect to observe one-magnon Raman scattering indicating longitudinal-mode magnetic excitations as in TlCuCl<sub>3</sub> [8] and KCuCl<sub>3</sub> [11].

#### IV. CONCLUSION

We measured the temperature dependence of the magnetic susceptibility and specific heat and the magnetic-field dependence of the magnetization of CuInVO<sub>5</sub>. An antiferromagnetically ordered state appears below  $T_N = 2.7$  K. We observed a  $\frac{1}{2}$  quantum magnetization plateau above 30 T at 1.3 K. An isolated antiferromagnetic spin- $\frac{1}{2}$  tetramer model with  $J_1 = 240$  and  $J_2 = -142$  K can closely reproduce the magnetic susceptibility above 30 K.

We were able to explain the magnetization curves using the interacting spin tetramer model with the effective intertetramer interaction  $J_{\text{eff}} = 30$  K. The value of the spin gap (singlet-triplet gap) is 17 K (1.5 meV) in the isolated spin tetramer. Detectable low-energy (on the order of 1 meV) longitudinal-mode magnetic excitations may exist in CuInVO<sub>5</sub>.

#### Acknowledgments

This work was financially supported by Japan Society for the Promotion of Science (JSPS) KAKENHI (Grant Nos. 23540396 and 15K05150) and by grants from National Institute for Materials Science (NIMS). M. Matsumoto was supported by JSPS KAKENHI (Grant No. 26400332). The high-field magnetization experiments were conducted under the Visiting Researcher's Program of the Institute for Solid State Physics (ISSP), the University of Tokyo. We are grateful to S. Matsumoto for sample syntheses and x-ray diffraction measurements.

---

[1] H. Tanaka, K. Goto, M. Fujisawa, T. Ono, and Y. Uwatoko, Magnetic ordering under high pressure in the quantum spin system  $\text{TlCuCl}_3$ , *Physica B* **329-333**, 697 (2003).

[2] A. Oosawa, K. Kakurai, T. Osakabe, M. Nakamura, M. Takeda, and H. Tanaka, Pressure-induced successive magnetic phase transitions in the spin gap system  $\text{TlCuCl}_3$ , *J. Phys. Soc. Jpn.* **73**, 1446 (2004).

[3] A. Oosawa, M. Ishii, and H. Tanaka, Field-induced three-dimensional magnetic ordering in the spin-gap system  $\text{TlCuCl}_3$ , *J. Phys.: Condens. Matter.* **11**, 265 (1999).

[4] T. Nikuni, M. Oshikawa, A. Oosawa, and H. Tanaka, Bose-Einstein condensation of dilute magnons in  $\text{TlCuCl}_3$ , *Phys. Rev. Lett.* **84**, 5868 (2000).

[5] H. Tanaka, A. Oosawa, T. Kato, H. Uekusa, Y. Ohashi, K. Kakurai, and A. Hoser, Observation of Field-Induced Transverse Néel Ordering in the Spin Gap System  $\text{TlCuCl}_3$ , *J. Phys. Soc. Jpn.* **70**, 939 (2001).

[6] K. Goto, M. Fujisawa, H. Tanaka, Y. Uwatoko, A. Oosawa, T. Osakabe, and K. Kakurai, Pressure-Induced Magnetic Quantum Phase Transition in Gapped Spin System  $\text{KCuCl}_3$ , *J. Phys. Soc. Jpn.* **75**, 064703 (2006).

[7] A. Oosawa, T. Takamasu, K. Tatani, H. Abe, N. Tsuji, O. Suzuki, H. Tanaka, G. Kido, and K. Kindo, Field-induced magnetic ordering in the quantum spin system  $\text{KCuCl}_3$ , *Phys. Rev. B* **66**, 104405 (2002).

[8] H. Kuroe, K. Kusakabe, A. Oosawa, T. Sekine, F. Yamada, H. Tanaka, and M. Matsumoto, Magnetic field-induced one-magnon Raman scattering in the magnon Bose-Einstein condensation phase of  $\text{TlCuCl}_3$ , *Phys. Rev. B* **77**, 134420 (2008).

[9] Ch. Rüegg, B. Normand, M. Matsumoto, A. Furrer, D. F. McMorrow, K. W. Krämer, H.-U. Güdel, S. N. Gvasaliya, H. Mutka, and M. Boehm, Quantum Magnets under Pressure: Controlling Elementary Excitations in  $\text{TlCuCl}_3$ , *Phys. Rev. Lett.* **100**, 205701 (2008).

[10] P. Merchant, B. Normand, K. W. Krämer, M. Boehm, D. F. McMorrow, and Ch. Rüegg, Quantum and classical criticality in a dimerized quantum antiferromagnet, *Nat. Phys.* **10**, 373 (2014).

[11] H. Kuroe, N. Takami, N. Niwa, T. Sekine, M. Matsumoto, F. Yamada, H. Tanaka, and K. Takemura, Longitudinal magnetic excitation in  $\text{KCuCl}_3$  studied by Raman scattering under hydrostatic pressures, *J. Phys.: Conf. Ser.* **400**, 032042 (2012).

[12] M. Matsumoto, B. Normand, T. M. Rice, and M. Sigrist, Field- and pressure-induced magnetic quantum phase transitions in  $\text{TlCuCl}_3$ , *Phys. Rev. B* **69**, 054423 (2004).

[13] M. Matsumoto, H. Kuroe, A. Oosawa, and T. Sekine, One-Magnon Raman Scattering as a Probe of Longitudinal Excitation Mode in Spin Dimer Systems, *J. Phys. Soc. Jpn.* **77**, 033702 (2008).

[14] J. Goldstone, A. Salam, and S. Weinberg, Broken Symmetries, *Phys. Rev.* **127**, 965 (1962).

[15] P. W. Higgs, Broken Symmetries and the Masses of Gauge Bosons, *Phys. Rev. Lett.* **13**, 508 (1964).

[16] S. Sachdev, *Quantum Phase Transitions Second Edition* (Cambridge University Press, Cambridge, U.K., 2011).

[17] D. Podolsky, A. Auerbach, and D. P. Arovas, Visibility of the amplitude (Higgs) mode in condensed matter, *Phys. Rev. B* **84**, 174522 (2011).

[18] M. Matsumoto, H. Kuroe, T. Sekine, and T. Masuda, Transverse and Longitudinal Excitation Modes in Interacting Multispin Systems, *J. Phys. Soc. Jpn.* **79**, 084703 (2010).

[19] M. Hase, M. Kohno, H. Kitazawa, O. Suzuki, K. Ozawa, G. Kido, M. Imai, and X. Hu, Coexistence of a nearly spin-singlet state and antiferromagnetic long-range order in quantum spin system  $\text{Cu}_2\text{Cd}_2\text{O}_6$ , *Phys. Rev. B* **72**, 172412 (2005).

[20] M. Hase, A. Dönni, V. Yu. Pomjakushin, L. Keller, F. Gozzo, A. Cervellino, and M. Kohno, Magnetic structure of  $\text{Cu}_2\text{Cd}_2\text{O}_6$  exhibiting a quantum-mechanical magnetization plateau and classical antiferromagnetic long-range order, *Phys. Rev. B* **80**, 104405 (2009).

[21] M. Hase, K. Nakajima, S. Ohira-Kawamura, Y. Kawakita, T. Kikuchi, and M. Matsumoto, Magnetic excitations in the spin- $\frac{1}{2}$  tetramer substance  $\text{Cu}_2^{114}\text{Cd}^{11}\text{B}_2\text{O}_6$  obtained by inelastic neutron scattering experiments, *Phys. Rev. B* **92**, 184412 (2015).

[22] T. Masuda, A. Zheludev, B. Grenier, S. Imai, K. Uchinokura, E. Ressouche, and S. Park, Cooperative Ordering of Gapped and Gapless Spin Networks in  $\text{Cu}_2\text{Fe}_2\text{Ge}_4\text{O}_{13}$ , *Phys. Rev. Lett.* **93**, 077202 (2004).

[23] T. Masuda, A. Zheludev, B. Sales, S. Imai, K. Uchinokura, and S. Park, Magnetic excitations in the weakly coupled spin dimers and chains material  $\text{Cu}_2\text{Fe}_2\text{Ge}_4\text{O}_{13}$ , *Phys. Rev. B* **72**, 094434 (2005).

[24] T. Masuda, K. Kakurai, M. Matsuda, K. Kaneko, and N. Metoki, Indirect magnetic interaction mediated by a spin dimer in  $\text{Cu}_2\text{Fe}_2\text{Ge}_4\text{O}_{13}$ , *Phys. Rev. B* **75**, 220401(R) (2007).

[25] T. Masuda, K. Kakurai, and A. Zheludev, Spin dimers in the quantum ferrimagnet  $\text{Cu}_2\text{Fe}_2\text{Ge}_4\text{O}_{13}$  under staggered and random magnetic fields, *Phys. Rev. B* **80**, 180412(R) (2009).

[26] M. Hase, K. M. S. Etheredge, S.-J. Hwu, K. Hirota, and G. Shirane, Spin-singlet ground state with energy gaps in  $\text{Cu}_2\text{PO}_4$ : Neutron-scattering, magnetic-susceptibility, and ESR measurements, *Phys. Rev. B* **56**, 3231 (1997). In this reference, the Hamiltonian is defined as  $\mathcal{H} = \sum_{i,j} 2J_{ij} \mathbf{S}_i \cdot \mathbf{S}_j$  instead of  $\mathcal{H} = \sum_{i,j} J_{ij} \mathbf{S}_i \cdot \mathbf{S}_j$  in the present paper.

[27] P. Moser, V. Cirpus, and W. Jung, CuInOVO<sub>4</sub> - Single Crystals of a Copper(II) Indium Oxide Vanadate by Oxidation of Cu/In/V Alloys, *Z. Anorg. Allg. Chem.* **625**, 714 (1999).

[28] The estimation of the magnetic specific heat strongly depends on the estimation of the lattice specific heat. There is no nonmagnetic isostructural compound for  $\text{CuInVO}_5$ . The magnetic specific heat probably remains up to a high  $T$  because of the low-dimensional spin system. We cannot determine whether the magnetic specific heat estimated on the basis of an assumption of the lattice specific heat is correct or not. Accordingly, we did not estimate the magnetic specific heat.

[29] M. Hase, I. Terasaki, and K. Uchinokura, Observation of the Spin-Peierls Transition in Linear  $\text{Cu}^{2+}$  (Spin- $\frac{1}{2}$ ) Chains in an Inorganic Compound  $\text{CuGeO}_3$ , *Phys. Rev. Lett.* **70**, 3651 (1993).

[30] M. Hase, I. Terasaki, Y. Sasago, K. Uchinokura, and H. Obara, Effects of Substitution of Zn for Cu in the Spin-

Peierls Cuprate,  $\text{CuGeO}_3$ : The Suppression of the Spin-Peierls Transition and the Occurrence of a New Spin-Glass State, *Phys. Rev. Lett.* **71**, 4059 (1993).

[31] M. Hase, I. Terasaki, K. Uchinokura, M. Tokunaga, N. Miura, and H. Obara, Magnetic phase diagram of the spin-Peierls cuprate  $\text{CuGeO}_3$ , *Phys. Rev. B* **48**, 9616 (1993).

[32] M. Hase, M. Kohno, H. Kitazawa, N. Tsujii, O. Suzuki, K. Ozawa, G. Kido, M. Imai, and X. Hu, 1/3 magnetization plateau observed in the spin-1/2 trimer chain compound  $\text{Cu}_3(\text{P}_2\text{O}_6\text{OH})_2$ , *Phys. Rev. B* **73**, 104419 (2006).

[33] M. Hase, M. Matsuda, K. Kakurai, K. Ozawa, H. Kitazawa, N. Tsujii, A. Dönni, M. Kohno, and X. Hu, Direct observation of the energy gap generating the 1/3 magnetization plateau in the spin-1/2 trimer chain compound  $\text{Cu}_3(\text{P}_2\text{O}_6\text{OD})_2$  by inelastic neutron scattering measurements, *Phys. Rev. B* **76**, 064431 (2007).